J Braz. Soc. Mech. Sci. Eng. (2014) 36:807–823
DOI 10.1007/s40430-014-0130-6

TECHNICAL PAPER

Investigations into the surface quality and micro-hardness in the ultrasonic machining of titanium (ASTM GRADE-1)

Jatinder Kumar

Received: 18 July 2013 / Accepted: 6 January 2014 / Published online: 23 January 2014

Abstract In the current study, the influence of various process parameters such as tool material, abrasive type, slurry grit size and power rating on the surface quality and the micro-hardness of the machined surface has been reported while machining pure titanium (ASTM Grade-I) using ultrasonic machining. Taguchi's robust design approach has been utilized for planning the experiments and optimizing the experimental results of surface roughness and micro-hardness. The surface topography of the machined samples revealed that the mode of material removal is related to the energy input rate. The mode of material removal may change from plastic deformation to brittle fracture under varied conditions of energy input rate. The hardness gradient has also been evaluated for selected process conditions and correlated with the energy input rate corresponding to each of the conditions.

Keywords Ultrasonic machining · Titanium · Surface quality · Micro-hardness · Taguchi method

Abbreviations

MRR	Material removal rate
TWR	Tool wear rate
SR	Surface roughness
S/*N*	Signal-to-noise ratio
DOE	Design of experiments
OA	Orthogonal array
SS	Sum of squares
MS	Mean square
DOF	Degrees of freedom
F	Fisher's ratio
P	Probability value
TQNL	Total normalized quality loss
MSNR	Multiple *S*/*N* ratio

1 Introduction

Ultrasonic machining is one of the non-traditional machining methods employed for machining hard (brittle and fragile) materials: semiconductors, Glass, quartz, ceramics, silicon, germanium, ferrites, etc. Titanium and its alloys attract a large number of industrial applications because of their distinguished characteristics such as higher strength and stiffness retained at higher temperatures, high tenacity coupled with superior resistance to corrosion and oxidation. However, these peculiar characteristics endorse titanium and its alloys in the category of difficult-to-machine materials with the conventional machining technology.

Because of this, the use of titanium and its alloys in industrial applications is becoming limited and is bound to face more resistance in coming time [1, 2]. The following problems have been reported in the conventional machining of titanium [3]:

– The thermal conductivity of titanium is much less as compared to steel and other ferrite metals; hence, there is severe heat concentration on the principal cutting edge and face of the tool. Moreover, the contact length at the tool–chip interface is very small. The temperature and shear stress concentration cause severe thermal damage and tool wear [4].

Technical Editor: Alexandre Mendes Abrao.

J. Kumar (✉)
Department of Mechanical Engineering, National Institute of Technology, Kurukshetra, India
e-mail: jatin.tiet@gmail.com

- Titanium is thermally and plastically unstable while machining. This produces non-uniform and highly localized shear strains in the chip forming serrated chips [5].
- The tool undergoes a consistent level of micro-fatigue load resulting from the fluctuations in the cutting force, which in turn, are caused by serrated chips being formed. This results in severe flank wear [6].
- The surface quality obtained is not acceptable while using a particular machining method.

Therefore, it is vital to establish cost-effective alternate machining methods for titanium and the related alloys. In recent times, many developments in the area of cutting tool fabrication using advanced tool materials such as carbides (both coated and non-coated), ceramics, stellite, poly-crystalline diamond (PCD) have been reported [3–5, 7]. However, none of the techniques making use of the advanced tool materials have ever been much successful in addressing the problems caused by the poor machinability of titanium effectively.

Many studies have been conducted for exploring the machinability of titanium and related alloys using non-conventional techniques such as laser beam machining, electro-discharge machining, wire EDM, etc. However, all of these viable techniques have exhibited their limitations [8–12]; in the context of deteriorated surface quality (at higher machining rates), poor dimensional accuracy or form accuracy and other undesirable effects post machining such as sub-surface thermal damage, recast layer formation and alternation of mechanical properties. These undesired changes in the surface integrity may reduce the effective life of the processed components. In case of titanium, the reduction in fatigue properties (after processing) is a major concern for the machinists. The fatigue characteristics of titanium components are dependant, to a large extent, on the generation of a compressive stress in the sub-surface by the impact of the tool during processing [4, 5, 13].

Ultrasonic Machining (USM) could be a viable alternative for exploring the machinability of titanium, as the process is known to be free from many of the problems associated with thermal-based processes mentioned above and the repeated action of the abrasive particles hammered by the tool yields a sub-surface compressive stress which can be helpful in obtaining good fatigue characteristics and prevent the loss of surface integrity [6, 14]. Recently, some of the reported studies have attempted to explore the machining performance of USM with titanium being work material [15–22]. However, the following critical issues are still pending to be explored.

1. Evaluation of the resulting change in the micro-hardness of the machined titanium samples as a consequence of the strain hardening of the work surface due to repeated grain impacts during machining.
2. Collective optimization of the surface quality and the micro-hardness of the machined surface (multi-response optimization of these two response variables).
3. Correlating the mode of material removal with the process conditions, particularly the energy input rate in the surface under machining, while considering titanium as work material.
4. Computation of the hardness gradient, i.e. the change in hardness of the machined surface with the depth, in a direction parallel to the direction of machining.

In present investigation, the focus has been on exploring all these critical issues in ultrasonic machining of pure titanium.

2 Literature review

USM is a non-thermal process and the machined surface is normally exempted from the undesired effects such as formation of carbon rich layer, residual stresses and the sub-surface thermal damage. Grit size of the abrasive slurry has been found to be the main factor governing the workpiece accuracy and surface roughness [1, 23–27]. Guzzo et al. [28] concluded that surface roughness is closely controlled by abrasive grain size alone. Kumar and Khamba [16] have also reported similar results. A decrease in abrasive grain size while machining with USM leads to lower values of surface roughness, apart from improving the dimensional accuracy of the drilled hole [15, 23, 27]. A better surface finish is also obtained on the bottom walls of the cavity. Dam et al. [29] reported that increased values of feed rate and depth of cut yield better surface quality. Kennedy and Grieve [1] and Koval'Chenko et al. [30] reported that the bottom surface of the drilled hole has a concave dish formation due to difficulty in feeding the slurry actively under the tool face, particularly at the centre. Komaraiah and Reddy [31] compared the performance of stainless steel, titanium and niamonic-80 tools for surface roughness of the glass workpiece while machining with USM. Results showed that tool materials with higher wear resistance (niamonic-80) gave better surface finish as they retain their shape and finish even under the repeated impact of abrasive particles.

Shaw [32] and Komaraiah et al. [27] have shown that surface quality improves while increasing the static feed force (load). The vibration of the tool in lateral direction is suppressed and the grit size gets reduced due to breakage and wear of particles, thereby controlling the production inaccuracies in the hole drilled. It was established by Komaraiah et al. [27] that workpiece materials possessing

higher values of the hardness/elastic modulus ratio involve inferior surface quality. The materials which observed higher material removal rate (MRR) were also reported to have higher surface roughness values. Dam et al. [29] concluded that the different work materials could be put in an ascending order in terms of the surface roughness obtained while they are ranked according to the metal removal rates observed while machining them. Therefore, enhancement in the productivity could only be obtained at the cost of the surface quality.

Sharman et al. [33] outlined the use of ultrasonic vibration-aided turning for machining of γ-titanium aluminide. The tool life and surface finish were reported to be improved due to very small magnitude of the cutting force, which was observed to be as less as only 12 % of that in conventional turning process. Aspinwall and Kasuga [34] reported the application of ultrasonic drilling in machining of titanium aluminide. The study was targeted at exploring the surface integrity of the work material using the tools made of polycrystalline diamond (PCD). The surface quality was found to be superior to other materials such as ceramics.

Singh and Khamba [21, 22] did research on the machining of titanium alloy (Ti-6Al-4 V) using static USM (no rotation of the tool). Results show that optimum surface quality was generated while using a stainless steel tool; slurry concentration of 25 % and slurry temperature equal to 27 °C. Dvivedi and Kumar [15] investigated surface quality in USM of titanium alloy (Ti-6Al-4 V). Results show that the best results for surface quality were obtained with H.C.S. tool; medium grit size (320 mesh) and low power rating of USM machine (40 %).

The current study is targeted at addressing the various issues described at the end of previous section while adopting ultrasonic machining as the processing technique for titanium.

3 Materials and methods

This study involves drilling of pure titanium (ASTM Grade-I) under varied and controlled experimental conditions created by combinations of different values of process parameters such as tool material, abrasive grit size, power rating of the machine and slurry material. The composition of the work material and important mechanical properties have been tabulated (Table 1). Tools were made of five different materials, representing a wide spectrum of mechanical characteristics such as strength, hardness and ductility. Four of the tools (made of high-speed steel, high-carbon steel, titanium and Ti alloy) were fabricated as a single, integral part on a heavy duty lathe machine. The cemented carbide tool was fabricated by brazing technique (using silver) as it was very difficult to turn the material due to its hardness. The designing of the different tools was done giving adequate consideration to the tool weight. Because the values of density for the different tool materials under consideration were significantly different, the dimensions of the each tool were determined in such a manner that the mass of each tool is almost equal (50 g). The tool geometry for the different tools used has been shown in Fig. 1, along with the three-dimensional pictorial representation of the tool. It was observed that the tool tip length could not be exceeded 20 mm; otherwise, it resulted in overstressing of the tool and premature failure due to fatigue. The workpiece was positioned under the tool using a fixture made in the shape of a gear (Fig. 2) which had a slot for holding the cylindrical shaped work sample. The fixture was placed on the magnetic work table and due to absence of cutting forces in USM, the simple arrangement of fixing the work sample was adequate and no problems related to shaking or withdrawal of the work sample (from its position) were encountered.

The experiments were conducted on an 'AP-500 model Sonic-Mill' ultrasonic machine (Sonic-Mill, Albuquerque, USA). The complete setup consisted of four sub systems: power supply; module unit; slurry re-circulating system and workpiece holder. The USM equipment used for this research has been depicted in Fig. 2, with all its components clearly marked. The surface roughness values were determined using "Perthometer" (Mahr, M4Pi). The surface roughness value (arithmetic mean, R_a) was measured at three different locations at the bottom flat of the hole

Table 1 Chemical composition and important properties of titanium and its alloy

Chemical composition (by wt %) of titanium (ASTM Grade-I)												
O	N	C	H	Fe	Ti	O	N	C	Fe	Al	V	Ti
0.17	0.025	0.08	0.015	0.25	99.0	0.15	0.05	0.06	0.25	5.8	4.1	89.3
Yield Strength	216 MPa					Ultimate strength	910 MPa					
Ultimate strength	332 MPa					Hardness	187 HV					
Hardness	115 HV					Density	4.4 g/cm^3					
Density	4.50 g/cm^3					Mod. of elasticity	114 GPa					
Mod. of elasticity	102 GPa					Fracture toughness	68 Mpam$^{1/2}$					

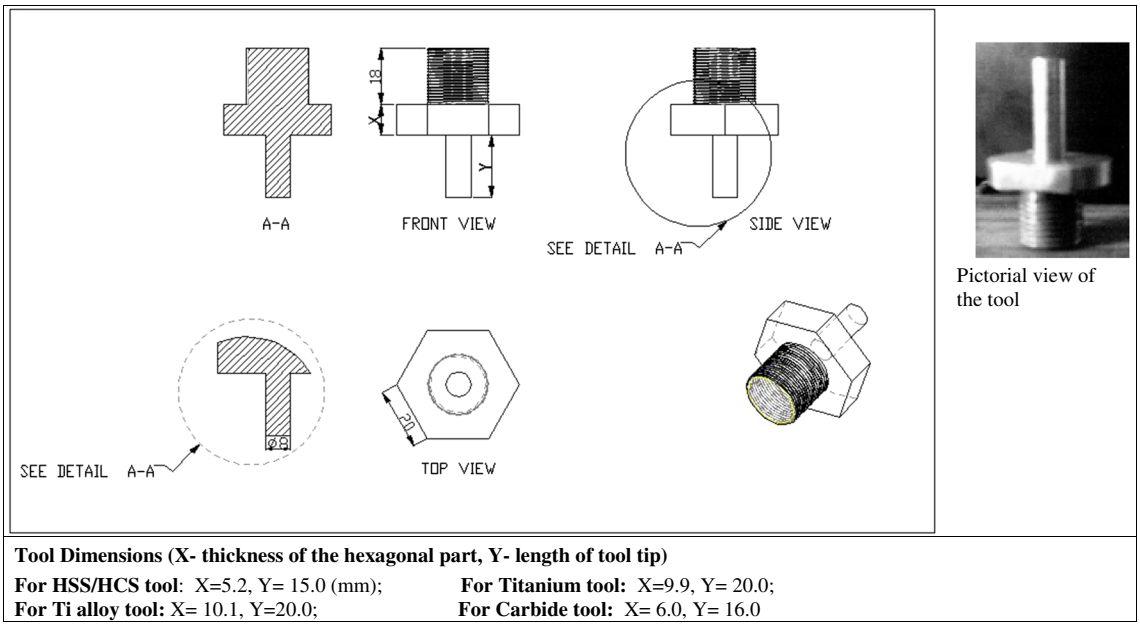

Tool Dimensions (X- thickness of the hexagonal part, Y- length of tool tip)

For HSS/HCS tool: X=5.2, Y= 15.0 (mm); **For Titanium tool:** X=9.9, Y= 20.0;
For Ti alloy tool: X= 10.1, Y=20.0; **For Carbide tool:** X= 6.0, Y= 16.0

Fig. 1 Tool geometry and pictorial representation

drilled and then the mean of these values was taken. In order to measure the hardness of the machined surface, the bottom flat of each hole was polished manually with diamond powder of very fine grit size (1,000) to obtain the required flatness as well as the high degree of finish. The hardness of the machined surface was then measured by micro-hardness tester under a static load of 500 g. The hardness values were also measured at three different locations on the bottom flat of each hole and then the mean of these values is computed. The experimental results for surface roughness and micro-hardness have been detailed in Table 2.

4 Experimentation and data collection

Taguchi's offline method of quality control involves application of standard arrays designated by Dr. Genichi Taguchi for designing the experiments and analyzing the resulting data as per standard methodology of robust design.

To decide the process parameters to be investigated in this research, a cause and effect diagram for surface quality in USM was constructed (Fig. 3. From the cause and effect diagram, following parameters were selected for investigation: tool material, abrasive type, slurry grit size and power rating of the USM equipment. These parameters were selected based on the findings of previous research reported in the literature [1, 2, 15, 21, 27], where these parameters have been termed as 'significant' for their effect on various responses (material removal rate, roughness). Other parameters such as static load, vibration frequency or slurry temperature could not be included due to machine set up limitations. Three different materials were used for preparing slurry namely; silicon carbide, aluminium oxide and boron carbide. Table 3 shows the various process parameters, whose influence was studied on the response variables—surface roughness and micro-hardness of the machined surface.

The levels of tool material factor were decided so as to obtain a wide range of mechanical properties such as ductility and hardness. Levels for the abrasive grit size factor were decided based on a 'preliminary experimental study' conducted using 'one factor at a time' approach.

While all other input parameters (such as power rating, abrasive material and tool) were kept fixed at their baseline levels, the grit size parameter was varied over a range, with a lowest value corresponding to mesh size of 600 and highest value being a mesh size of 100. Five different values were tried for grit size; with a mean mesh size of 100, 220, 320, 500 and 600 to assess the impact of the grit size on surface roughness. From the experimental results (Fig. 4), three levels of grit size parameter were selected for the final experimentation—220, 320 and 500. The levels of power rating factor were also chosen using the similar approach, by varying the power rating in the range of 100–400 W. The baseline level was fixed at 100 W and the further increments of 100 W were made in the power input while keeping all other parameters unchanged.

To contain the impact of possible noise factors such as variations in the abrasive slurry concentration, change in

Fig. 2 Detailed representation of USM apparatus used

tool shape (at the face) and abrasive particles wear; the following measures were taken:

1. The tool face was ground after every experiment to restore the original shape at the cross-section, as a concave dish formation happened due to inadequate flow of slurry under that area of the tool. Moreover, the roughness of the tool face was kept at a target value of 5 μm as the roughness of the tool face has a significant effect on the surface quality of the drilled hole [35].
2. The abrasive slurry was prepared using fresh, unused abrasive materials and in a large volume (about 30 litres), with a concentration of 25 % by volume to avoid any significant variations in the concentration during machining. Also, it was decided to replace the entire volume of slurry after a running time of 24 h to avoid the possibility of performing the experimentation with worn out abrasive particles. The time for the completion of an experiment may range from 20 min to 4 h, depending upon the values of the input parameter corresponding to the experiment. It has been observed from the previous research reported in the literature [1, 15, 21, 27] that the abrasive wear is not significant for machining time of 24 h. Moreover, the USM equipment manufacturer (Sonic-Mill, USA) had also recommended the replacement of slurry after a machining time of 24 h.
3. Three replications of the entire experiment, consisting of 54 experimental runs in total, were performed and the experimental runs were performed in a completely randomized fashion to average out the effect of any more noise factors acting.

In this study, Taguchi's L-18 orthogonal array (in modified form) was used for planning and designing of the experiments. The degrees of freedom of L-18 array (17 DOF) are adequately enough for the problem under consideration, which involves a total of 10 degrees of freedom when all input parameters are considered. As the tool material factor was having five levels, it was assigned to the first column of the array (Table 4) which could accommodate six levels otherwise. Making a duplicate allocation of tool 1 (HCS tool) to the last three experimental runs (Table 4) does not affect the orthogonality of the array used [36]. The next column was assigned to 'abrasive' factor. Remaining factors were assigned to columns 3 and 4 in the similar fashion. All of these factors have three levels each. It is not possible to investigate any interaction effects while applying L-18 array for designing the experiments [36], as the interactions are confounded with the main effects of various parameters. Moreover, from a previous research reported by author [16], none of the interactions were found to be statistically significant for their effect of surface quality while machining titanium with USM. Thus, the interactions among the parameters were omitted and L-18 array was used to optimize the amount of resources required for the experimentation.

According to the experimental design matrix (Table 4), three holes of diameter 8 mm and depth 2 mm were drilled (for each experiment) in the titanium work samples, which were fabricated by parting operation on a heavy duty lathe machine. In Table 4, the values of the input factors have been assigned a code, depending on the magnitude of the value assigned to the parameter for a particular level. The lowest level of a parameter is assigned a coded value of -1, whereas the intermediate level is given a coded value of 0 and the highest level is assigned a value of $+1$.

Table 2 Experimental results

Experiment no.	Roughness, R_a (μm)			Average SR (μm)	*S/N* ratio (dB)	Micro-hardness (HV)			Average micro-hardness (HV)	Hardness gain[a]	*S/N* ratio (dB)
	R1	R2	R3			R1	R2	R3			
1	0.98	0.85	0.92	0.92	0.74	154	147	150	151	36	43.54
2	1.18	1.05	1.24	1.16	−1.28	145	151	145	147	32	43.34
3	0.70	0.75	0.52	0.66	3.56	166	175	162	168	53	44.48
4	1.17	0.82	1.10	1.03	−0.35	144	152	149	148	33	43.42
5	1.20	1.18	1.32	1.23	−1.83	139	134	146	140	25	42.89
6	0.64	0.60	0.53	0.59	4.56	183	174	170	176	61	44.88
7	0.68	0.72	0.50	0.63	3.83	168	173	164	168	53	44.52
8	0.73	0.87	0.90	0.83	1.56	150	160	155	155	40	43.80
9	2.26	1.90	2.14	2.10	−6.47	135	137	140	137	22	42.75
10	0.56	0.68	0.75	0.66	3.51	175	178	162	172	57	44.67
11	0.64	0.78	0.60	0.67	3.38	160	154	156	157	42	43.90
12	0.86	0.85	0.80	0.84	1.54	145	153	151	150	35	43.50
13	0.97	1.04	1.12	1.04	−0.38	151	145	140	145	30	43.23
14	0.66	0.60	0.75	0.67	3.44	157	165	162	162	47	44.15
15	1.70	1.84	1.67	1.74	−4.80	140	145	148	144	29	43.18
16	0.66	0.77	0.83	0.75	2.42	149	157	152	153	38	43.67
17	2.24	2.18	2.29	2.24	−6.99	131	130	133	131	16	42.37
18	0.73	0.77	0.92	0.81	1.82	158	167	155	160	45	44.07

[a] Initial work hardness = 115HV

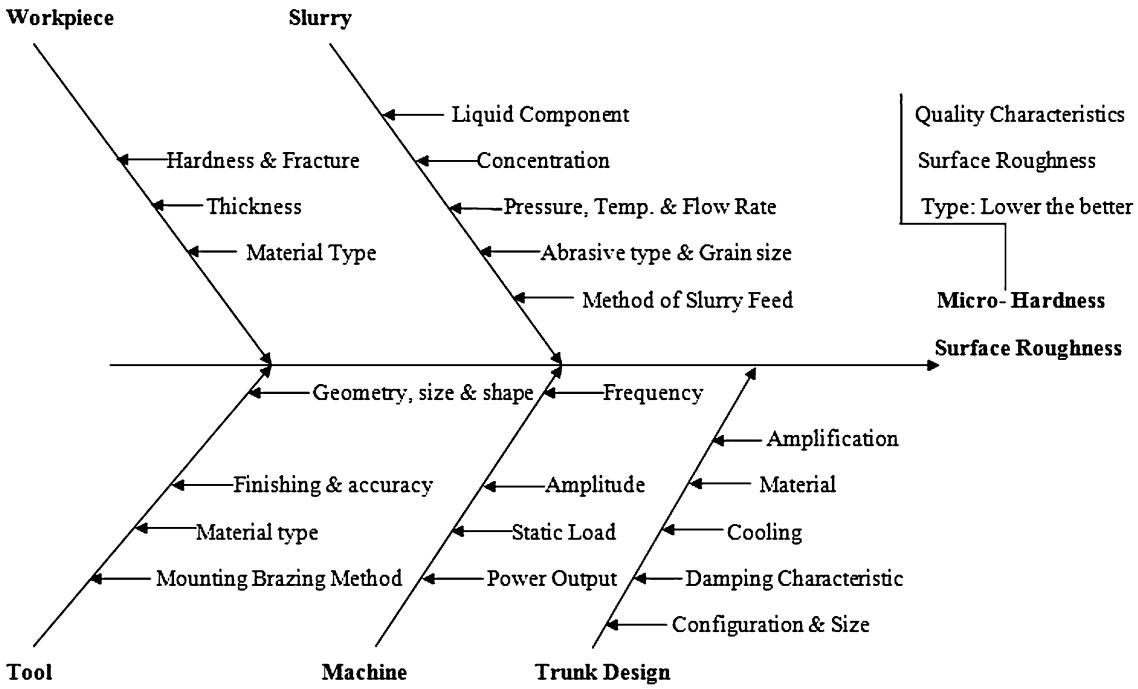

Fig. 3 Cause and effect diagram for surface quality in USM

Table 3 Process parameters and their values (with coded units)

Symbol	Parameter	Level 1	Level 2	Level 3	Level 4	Level 5
A	Tool material	HCS (−2)	HSS (−1)	Titanium (0)	Ti alloy (+1)	Carbide (+2)
B	Abrasive type	Alumina (−1)	SiC (0)	Boron carbide (+1)		
C	Grit size (mesh)	220 (+1)	320 (0)	500 (−1)		
D	Power rating	100 W(−1)	250 W(0)	400 W(+1)		
Constant parameters						
Frequency of vibration	20 kHz					
Static load	1.63 kg					
Amplitude of vibration	25.3–25.8 μm					
Depth of cut	2 mm					
Thickness of workpiece	10 mm					
Tool geometry	Straight cylindrical (with diameter 8 mm)					
Slurry concentration	25 % (by volume)					
Slurry temperature	28 °C (ambient room temperature)					
Slurry flow rate	36.4×10^3 mm^3/min					

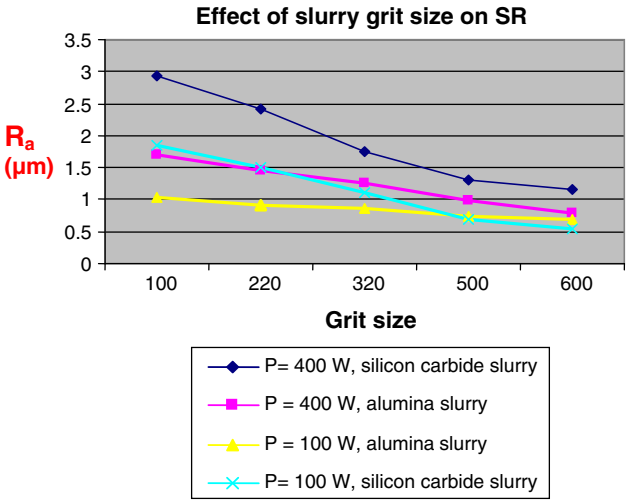

Fig. 4 Effect of slurry grit size on surface roughness (Tool: HCS)

5 Results and discussions

Taguchi's DOE methodology encourages the use of a statistical index known as 'Signal-to-noise (*S/N*) ratio'. *S/N* ratio represents the variability (in the experimental data) caused by the action of the predominant noise factors. By maximizing the value of *S/N* ratio, the variability in the machining performance may be minimized. In the current study, lower values of both response variables (roughness, hardness) are desirable. The *S/N* response most suited for this condition is 'lower-the-better' type, which is given by following relation [36].

$$\eta = -10\log_{10}\left\{\frac{1}{n}\cdot\sum_{1}^{n} y_i^2\right\} \quad (1)$$

Table 4 Experimental design based on L-18 OA

Experiment no.	A: tool material	B: abrasive	C: grit size	D: power rating
1	−2	−1	+1	−1
2	−2	0	0	0
3	−2	+1	−1	+1
4	−1	−1	+1	0
5	−1	0	0	+1
6	−1	+1	−1	−1
7	0	−1	0	−1
8	0	0	−1	0
9	0	+1	+1	+1
10	+1	−1	−1	+1
11	+1	0	+1	−1
12	+1	+1	0	0
13	+2	−1	0	+1
14	+2	0	−1	−1
15	+2	+1	+1	0
16	−2	−1	−1	0
17	−2	0	+1	+1
18	−2	+1	0	−1

where y_i represents a particular value of response i and n the number of replications used.

5.1 Surface roughness

Figure 5 depicts the dependence of surface roughness on the input process parameters investigated in the study. It could be seen that the tool material parameter is

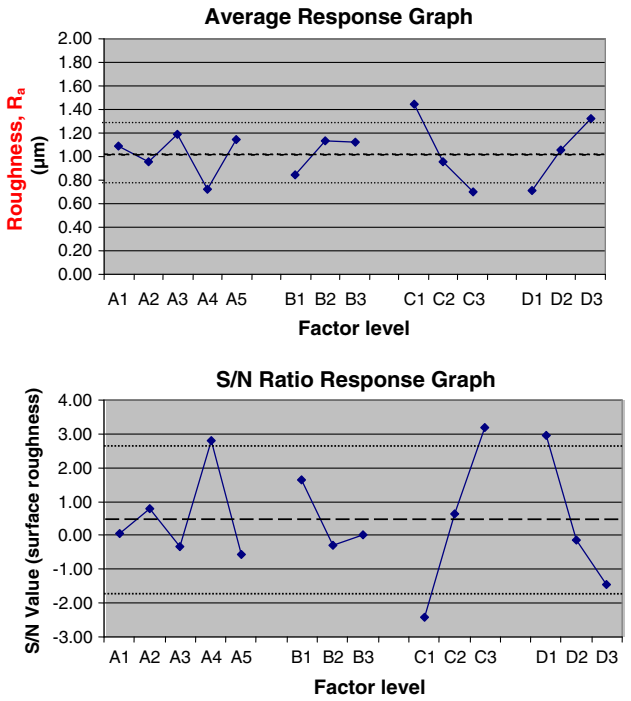

Fig. 5 Effects of process parameters on surface roughness (raw data and *S/N* ratio)

responsible for causing an appreciable change in the surface quality obtained under controlled experimental conditions, which is in agreement with the findings of other investigators [15, 16, 27, 28, 37]. The higher values of surface roughness for cemented carbide and high-carbon steel tools also indicate the presence of a strong correlation between surface quality and MRR, as the MRR observed while using these tool materials was found to be reasonably higher than other tool materials [16]. Use of a harder tool such as cemented carbide or high-carbon steel results in more indentation of the abrasive grain inside the work surface (for every impact) as compared to the tool surface which leads to creation of larger and deeper micro-cavities on the work surface, generating higher roughness [31, 35].

Alumina (as abrasive) has shown best results for surface quality. However, the difference between the performance of silicon carbide and boron carbide abrasives is only marginal. The superior performance of alumina could be based on its 'softness' or the least value of hardness in all the abrasives investigated in the study. Because of the low knoop hardness, use of alumina results in formation of smaller sized micro-cavities which controls the surface roughness.

The surface finish has been found to be deteriorated while the grit size of the abrasive slurry is increased (Fig. 5). This finding is in agreement with the outcomes of previous studies reported in the literature [15, 20–22, 28]. Bigger particles are able to gather more momentum from the vibrating tool and hence produce rapid micro-fracturing at the work surface; thereby quality of the machined surface is deteriorated. The abrasive particles movement is not confined to only the longitudinal gap between the tool and work, it also happens in the lateral direction (across the tool face). While the particle size is increased, the frictional force in the lateral direction increases and as the machining is continued, the movement of the abrasive grains in the deep downward direction results in non-uniform wear across the lateral interface. This increases the surface roughness and the finish is compromised.

It could be observed from Fig. 5 that increasing the input power results in a sharp increment in surface roughness. This can also be observed from Fig. 4, where using the same abrasive with higher power level brings a twofold increase in surface roughness. The abrasive particles striking on the work surface with extremely high momentum remove larger chunks of material, thereby increasing the surface roughness [16, 38–40].

It can be concluded from Table 5 that only slurry grit size and power rating factors are statistically significant for their effect on surface quality while machining titanium with USM. The percent contribution for slurry grit size has been found to be the highest among all the factors (41.5 %) whereas power rating comes next (26.2 %). Remaining factors can be termed as relatively insignificant for surface roughness. The *S/N* results (Table 6) indicate that slurry grit size has highest percent contribution (44.0 %) followed by power rating (28.8 %) for their effect on surface quality. The other two factors (tool material and abrasive type) have been found to be insignificant as far as *S/N* response is concerned. Hence, it can be concluded that "While machining titanium (ASTM Grade-I) with USM, input parameter settings of ultrasonic power rating at 100 W, with titanium alloy tool and aluminium oxide slurry with a fine grit size of 500 have given the optimum results for

Table 5 ANOVA results for surface roughness (raw data)

Source	*df*	Seq. SS	Adj. SS	Adj. MS	*F*	(%P)
Tool	4	1.31	1.31	0.33	6.42**	10.3
Abrasive	2	0.99	0.99	0.50	9.72**	7.8
Grit Size	2	5.30	5.30	2.65	51.80*	41.5
Power Rating	2	3.33	3.33	1.67	32.64*	26.2
Error	43	1.40	1.40	0.032	14.2	
Total	53	12.30				

$F_{tab} = F(4,43) = 2.60$; $F(2,43) = 3.21$

Order of significance:

1. Grit size 2. power rating 3. abrasive type 4. tool

df degrees of freedom, *Seq. SS* sequential sum of squares, *Adj. MS* adjusted mean square error

% P percent contribution. F_{tab} value is obtained from statistical tables

Table 6 ANOVA results for surface roughness (*S/N* data)

Source	*df*	Seq. SS	Adj. SS	Adj. MS	*F*	(%P)
Tool	4	23.147	23.147	5.787	1.81	10.8
Abrasive	2	12.728	12.728	6.364	1.99	6.0
Grit Size	2	93.927	93.927	46.963	14.68*	44.0
Power rating	2	61.516	61.516	30.758	9.62*	28.8
Error	7	22.392	22.392	3.199	10.4	
Total	17	213.710				

$F_{tab} = F(4,43) = 2.60$; $F(2,43) = 3.21$

Order of significance:

1. Grit size; 2. power rating; other factors are insignificant.

Table 7 Macro-model for surface roughness

Optimization of surface roughness	Confirmatory results for surface roughness
	R1 R2 R3 mean (μm)
Tool material: titanium alloy	0.37 0.30 0.28 0.32
Abrasive material: alumina	Predicted value: 0.36
Grit size 500 (fine)	Confidence interval (95 %)
Power rating 100 W (20 %)	$0.12 < \mu_{\text{surface roughness}} < 0.60$

surface quality". The percentage contributions of various factors towards the variation of surface roughness have been depicted in Fig. 6 for raw data and *S/N* data.

5.2 Prediction of the optimized value for surface roughness

For surface roughness only two factors have been found to be significant: power rating, grit size (Table 5). Hence other factors have been omitted in estimation of optimum value for surface roughness.

$\mu_{SR} = (\mu C3 + \mu D1) - (\mu) = 0.36$ μm.

where μ = mean of the population for surface roughness = 1.03.

$\mu C3 = 0.68$, $\mu D1 = 0.72$ (Table 5).

For calculation of CI_{CE}, the following equation [36] has been used:

$$CI_{CE} = \sqrt{F_{\alpha}(1, f_e)\left\{\frac{1}{n_{eff}} + \frac{1}{R}\right\}V_e} \quad (2)$$

$F_{\alpha}(1, f_e)$ = the F-ratio at a confidence level of (1-α) against DOF 1 and error degrees of freedom f_e (for surface roughness, $f_e = 43$, so F_{α} is 4.05).

V_e = error variance for surface roughness.

$V_e = 0.032$ (Table 6).

$$n_{eff} = \frac{N}{1 + \text{Total DF involved in estimation of mean}} \quad (3)$$

N = total number of experiments.

$n_{eff} = 54/(1 + 10) = 4.9$

$R = 3$ (no. of replications for each trial).

Putting all the values in equation (2) yields;

$CI_{CE(SR)} = \pm 0.24$.

The 95 % confidence interval for μ_{SR} is,

$CI_{CE(SR)} = 0.12 < \mu_{SR} < 0.60$.

The optimized value of surface roughness and the confidence interval (at 95 % level) have been given in Table 7. Three confirmation experiments were conducted at the optimized process setting represented by titanium alloy tool in conjunction with a soft abrasive (alumina) and very fine particle size (500 mesh). The mean value of the roughness obtained from the confirmation experiment is found to be well inside the limits represented by confidence interval (Table 7) thus validating the optimized results.

5.3 Micro-hardness and its correlation with surface quality

To assess the contribution of various factors towards the variation in micro-hardness, ANOVA for both raw data as well as *S/N* data have been performed (Tables 8, 9). It could be concluded that the micro-hardness after machining is strongly dependant on the input power and slurry grit size used for machining. Slurry grit size emerges as the most significant factor with a percent contribution of 42 % followed by power rating (26.5 %) and abrasive type (9.8 %). ANOVA for *S/N* data also depicts similar results

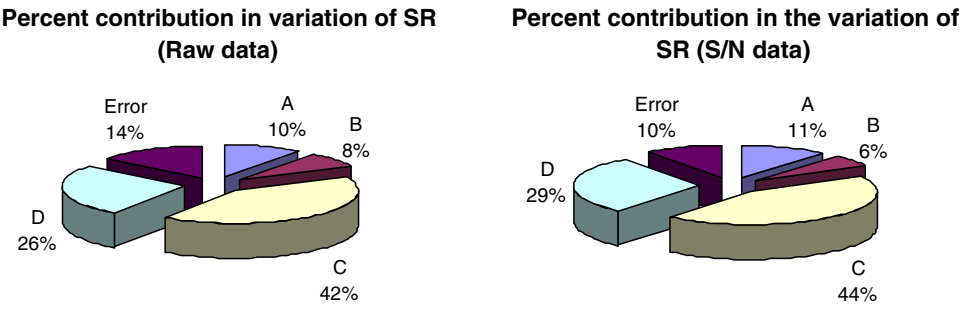

Fig. 6 Percent contributions of various input factors for SR

Table 8 ANOVA results for Micro-hardness (raw data)

Source	*df*	Seq. SS	Adj. SS	Adj. MS	*F*	(%P)
Tool	4	478.48	478.48	119.62	2.65	5.6
Abrasive	2	666.04	666.04	333.02	7.38*	9.8
Grit size	2	3,431.81	3,431.81	1,715.91	38.00*	42.3
Power rating	2	1,997.48	1,997.48	998.74	22.12*	26.5
Error	43	1,941.61	1,941.61	45.15	15.8	
Total	53	8,515.43				
$F_{tab} = F(4,43) = 2.60$; $F(2,43) = 3.21$						
Order of significance						
1. Grit size; 2. power rating; 3. abrasive						

Table 9 ANOVA results for Micro-hardness (*S/N* data)

Source	*df*	Seq. SS	Adj. SS	Adj. MS	*F*	(%P)
Tool	4	0.4959	0.4959	0.1240	0.78	6.2
Abrasive	2	0.7057	0.7057	0.3528	2.21	8.8
Grit Size	2	3.5949	3.5949	1.7974	11.24*	45.0
Power rating	2	2.1783	2.1783	1.0892	6.81*	27.2
Error	43	1.1195	1.1195	0.1599	12.8	
Total	53	8.0943				
$F_{tab} = F(4,43) = 2.60$; $F(2,43) = 3.21$						
Order of significance						
1. Grit size; 2. power rating; other factors are insignificant.						

where both grit size and power rating emerge as significant factors with percent contributions of 45.0 and 27.2 %. The variation in the micro-hardness with process conditions can be explained from the energy considerations. In USM, the energy input to the work surface per impact is a function of the various operating parameters such as amplitude of vibration, slurry grit size, power rating of the USM machine, etc. The energy input rate can be increased by increasing the coarseness of the slurry or the power rating. Increasing the coarseness of the slurry leads to higher momentum of abrasive particles which results in stronger impacts on the work surface, increasing the energy input rate. Abrasive hardness does not influence the energy input rate, hence it does not produce significant variation in micro-hardness.

The hardness of the machined surface has been found to be correlated with the surface quality obtained in USM of titanium. The process conditions that result in fine surface quality (lower roughness) correspond to lower values of the energy input. Under the conditions of low energy input per impact (hence per unit time), the work surface experiences plastic deformation for longer sustained time period, which leads to more work hardening and hence the larger gain in hardness after machining (experimental runs 6, 7, 8, 11, 14, 16, 18). Also, the tools that possess higher toughness and low elastic modulus (such as titanium, titanium alloy tools), contribute more towards the sustained plastic deformation of the work surface, leading to the higher hardness of the work surface after machining (experimental runs 7, 10). Hence, the process settings that result in better machining performance in terms of surface quality also result in more work hardening of the machined surface, thereby promoting a large increment in the hardness of the work material after machining with USM (Table 2).

The correlation of surface roughness and micro-hardness has been established through quadratic regression (Fig. 7). The best fitting line for prediction of micro-hardness over a large range of surface roughness was discovered using MINITAB 15 software. The quadratic regression equation for the least squares line is

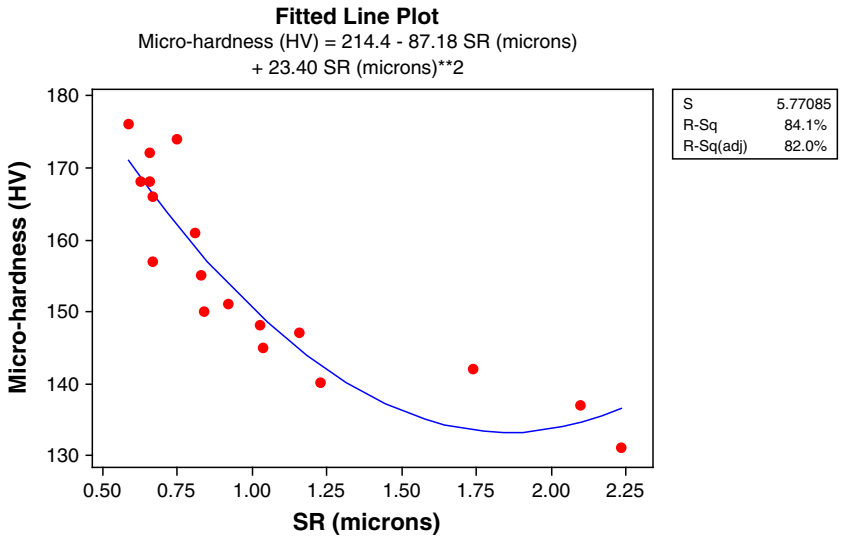

Fig. 7 Correlation between surface roughness and micro-hardness

$$H = 214.4 - 87.18\,S + 23.40\,S^2 \quad (4)$$

H = micro-hardness value (HV).
S = surface roughness (microns).

The direct estimation of the micro-hardness of ultrasonically machined samples saves invaluable time as well as the effort of the investigator as it is very cumbersome to prepare the machined titanium components for further metallographic testing. The surface preparation for titanium generally involves use of mechanical, electrolytic or chemical polishing methods in combination with precision diamond grinding [6]. Moreover, the grinding and polishing rates for titanium are much lower than other metals due to its high sensitivity to surface damage [41]. Under these conditions, the direct estimation of micro-hardness could be a cost-effective alternative.

5.4 Multi-objective optimization using Taguchi's approach

There are many techniques reported in the available literature on statistical optimization of manufacturing methods, namely utility concept, desirability function, principal component analysis-based methods (such as grey relational analysis, TOPSIS) and many unconventional optimization techniques such as genetic algorithm (GA), Artificial neural network (ANN), etc. However, this investigation would make use of a standard Taguchi's approach, widely known as 'Loss-function' for multi-objective optimization of the two responses investigated (roughness, micro-hardness). Taguchi's approach to optimization has been widely employed for solution of practical problems associated with optimization, both in academic as well as industrial domain. This technique stresses the computation of 'Loss Function' for each characteristic (response in this case) and subsequently, the minimization of the collective loss; taking into account the loss function of the individual responses. Thus, this approach is expected to yield the results that would enable a machinist (end user) to minimize the deviations from the desired performance level under the unfavourable operating conditions (involving noise), which would eventually lead to better, robust process performance.

In order to achieve multi-objective optimization of surface roughness and micro-hardness, the quality loss for each quality characteristic has been computed. The quality loss is represented by mean square deviation function (MSD). MSD represents the deviation between the experimental value and the desired value. In present investigation, both characteristics (roughness and micro-hardness) are lower-the-better type. MSD for both characteristics has been computed using the following relation:

$$\text{MSD} = y_1^2 + y_2^2 + y_3^2 + y_n^2/n \quad (5)$$

where y_1, y_2, y_3, y_n represent the value of the response for a particular experimental run and n the number of replications. The quality loss values for each quality characteristic have been depicted in Table 10.

Table 10 Computational results for MSNR

Experiment no.	Quality loss		Normalized quality loss		Total normalized quality loss and multi-response *S/N* ratio	
	SR	Micro-hardness	SR	Micro-hardness	TQNL	MSNR (dB)
1	0.843	22,608	0.169	0.732	0.450	3.467
2	1.343	21,617	0.268	0.699	0.483	3.160
3	0.443	28,141	0.089	0.911	0.500	3.010
4	1.083	22,013	0.216	0.712	0.464	3.334
5	1.525	19,531	0.305	0.632	0.468	3.297
6	0.350	30,888	0.070	1.000	0.535	2.716
7	0.410	28,349	0.082	0.918	0.500	3.010
8	0.700	24,041	0.140	0.778	0.459	3.381
9	4.433	18,864	0.887	0.610	0.748	1.260
10	0.446	29,517	0.892	0.955	0.923	0.347
11	0.460	24,550	0.092	0.795	0.443	3.535
12	0.700	22,411	0.140	0.725	0.432	3.645
13	1.090	21,082	0.218	0.682	0.450	3.467
14	1.120	26,039	0.224	0.843	0.533	2.720
15	3.020	20,843	0.604	0.675	0.640	1.938
16	0.573	23,318	0.115	0.755	0.435	3.610
17	5.000	17,250	1.000	0.558	0.779	1.084
18	0.656	25,626	0.131	0.830	0.480	3.187

The normalized quality loss has been determined using the following relation [36].

$$y_{ij} = L_{ij}/L_{im} \tag{6}$$

where y_{ij} represents the normalized quality loss, L_{ij} the quality loss for the *ith* quality characteristic at the *jth* run in the experimental design matrix and L_{im} the maximum quality loss for *ith* quality characteristic among all the experimental runs. The normalized quality loss values for each quality characteristic are shown in Table 10.

The total normalized quality loss has been determined using following formula.

$$Y_j = \sum z_i y_{ij} (i \text{ ranges from 1 to } k) \tag{7}$$

where Y_j represents the total normalized quality loss, y_{ij} the normalized quality loss for the *ith* quality characteristic at the *jth* run, z_i the weighting factor for the ith quality characteristic and k the number of quality characteristics. Here $k = 2$ and assuming weighting factor z for SR and micro-hardness as 0.5 and 0.5 (giving equal weightage), the total normalized loss (TQNL) has been computed and tabulated in Table 10.

Table 11 Average Effects of factors on MSNR

Factors	Mean MSNR (dB)				
	Level 1	Level 2	Level 3	Level 4	Level 5
Tool	2.92	3.116	2.550	2.509	2.708
Abrasive	2.873	2.863	2.626	–	–
Grit size	2.436	3.294	2.631	–	–
Power rating	3.106	3.178	2.078	–	–

The multi-response *S/N* ratio (MSNR) as given in Table 10 has been determined from the following formula [36].

$$\mathcal{E}_j = -10 \log_{10}(Y_j) \tag{8}$$

The average effect of each factor on multiple quality characteristics has been tabulated in Table 11. The average effect is determined by the ratio of sum of all *S/N* ratios corresponding to a factor at particular level to number of repetitions of factor level. The average effects have been plotted in Fig. 8. The optimum combination from Fig. 14 has been identified as A2B1C2D2.

The optimal value of multi-response *S/N* ratio has been predicted using MINITAB 16 software. Also, the optimal values of roughness and micro-hardness at the optimum combination (A2B1C2D2) have been predicted. The predicted optimal values have been summarized in Table 12. Three confirmatory experiments were performed at the optimum combination and the experimental values have been found to be quite close to the predicted values (Table 12). The improvement in multi-response *S/N* ratio at the optimized condition over the initial setting has been found to be 0.62 dB. The values of roughness and micro-hardness at the optimal combination are 0.70 μm and 143 HV in comparison to 0.92 μm and 151 HV for initial setting of parameters.

6 Hardness profile of machined samples

To analyze the change in the hardness of the machined titanium samples with the depth (sub-surface effect), three samples machined at the process settings corresponding to

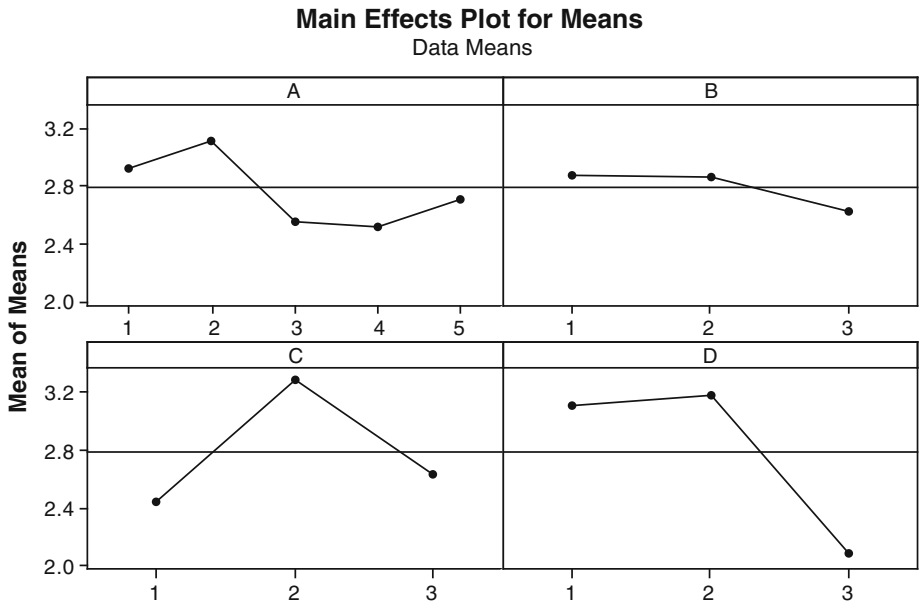

Fig. 8 Mean effects plot for multi-response *S/N* ratio

Table 12 Predicted optimal values for SR and micro-hardness

	Initial setting	Optimal values	
		Predicted	Experimental
Roughness	A1B1C1D1	A2B1C2D2	A2B1C2D2
Hardness	0.92	0.70	0.75
MSNR (dB)	151	143	141
	3.467	4.08	4.14

experiment trial no. 6, 12 and 9 were selected, to compare the effects of low energy input rate, moderate energy input rate and high energy input rate on the hardness profile.

Each of the three samples was cut to expose a cross-section at which the depth of the strain-hardened surface could be analyzed for micro-hardness test. Holes of larger size (20 mm) were cut at the selected experimental conditions (experiment no. 6, 9 and 12) in the titanium samples to a depth of cut of 3 mm. Thereafter, the sample was cut along the centre of the drilled hole in a direction perpendicular to the thickness of the workpiece using a diamond blade saw.

The next step was to polish the sample (at the required cross-section) to obtain a scratch-free and 'mirror like' finish so that the micro-hardness test could be performed with accuracy. The samples were polished using a very fine particle size alumina powder in aqueous solution. Final polishing was done on the polisher using silica suspension for even a better and smooth finish.

To measure the micro-hardness, the samples were placed inside the microscope and the measurements were made using the Vickers micro-hardness scale. First observation was taken on the bottom flat of the drilled hole, near the edge of the exposed cross-section. Subsequent measurements were taken along the depth of the exposed cross-section in increments of approx. 50 μm in dimension along the depth, up to a depth of 250 μm. The results depicting the variation of hardness with the sub-surface depth have been plotted in Fig. 9.

The following observations could be made from Fig. 9 (hardness profile).

1. At low energy input setting (Experiment No. 6), the effect of strain hardening lasts to a sub-surface depth of about 150–200 μm. There is a sharp decline observed in the hardness of the strain-hardened layer after reaching a depth of 50 μm. However, at a depth of 200 μm, and thereafter, the hardness of the sub-surface layers becomes equal to the hardness of un-machined sample (115 HV).
2. For moderate energy input setting (Experiment No. 12) as well as high energy input setting (Experiment No. 9), the trend for the hardness is almost same. In both cases, a gradual, consistent decline in hardness is observed along the sub-surface depth. The only difference is that in case of high energy input setting, the strain-hardening effect can be observed for a larger depth, in the range of 150–200 μm.

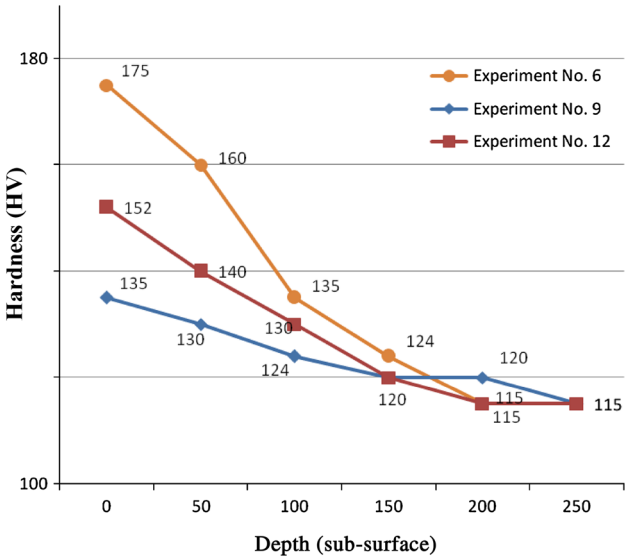

Fig. 9 Hardness profile of machined titanium samples

7 Microstructure analysis of machined samples

The machined samples were etched with Kroll's reagent (2 % HF, 10 % HNO_3, 88 % distilled water) and thereafter the microstructures of the machined surface were obtained using scanning electron microscope (SEM) at a fixed level of magnification—1,500×.

The material removal in a mechanical energy-based process such as ultrasonic machining has been discovered to occur by brittle fracture or micro-chipping of the work surface through a mechanism of micro-crack propagation followed by rapid interaction [39, 40]. However, even under these conditions, the chip formation may happen by plastic flow provided that the depth of cut is maintained at a level that is appreciably low [29, 42]. Hence, the mode of metal removal may be micro-fracturing of the work surface or consistent plastic deformation depending on the value of the depth of cut or metal removal rate used. The analysis of the microstructures (under different experimental configurations) has been undertaken to check the applicability of above-mentioned facts in USM of titanium.

Figures 10, 11, 12, 13, 14, 15 represent the microstructures of the work surface after machining with USM. It could be well observed that the experimental conditions that correspond to higher levels of energy input rate (Experiment No. 5, 13) involve realization of purely brittle

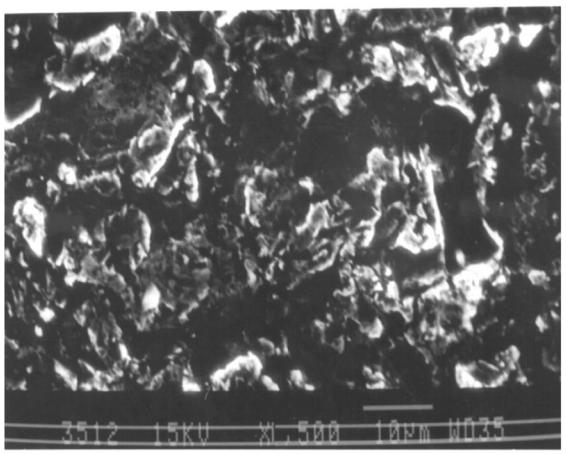

Figure 10 [Exp. No. 5]

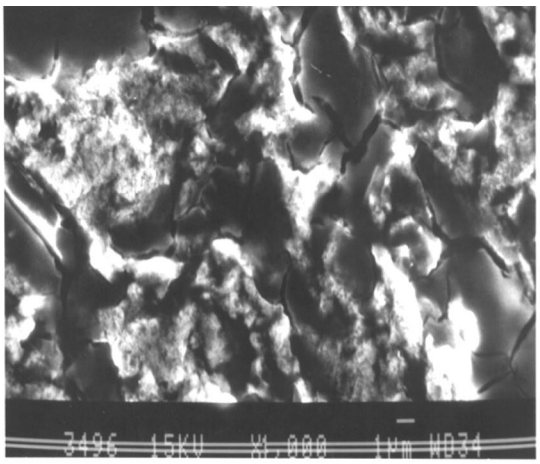

Figure 11 [Exp. No. 13]

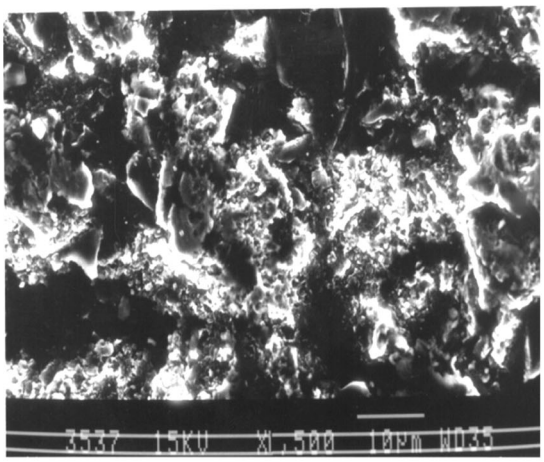

Figure 12 [Exp. No. 2]

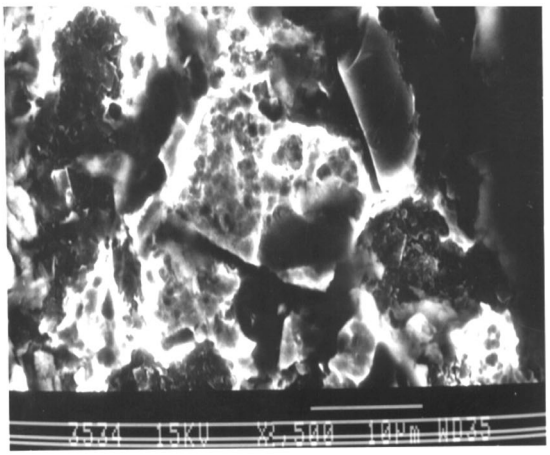

Figure 13 [Exp. No. 8]

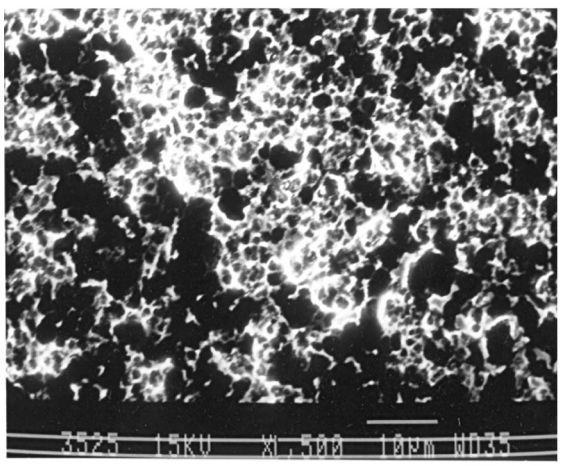

Figure 14 [Exp. No. 1]

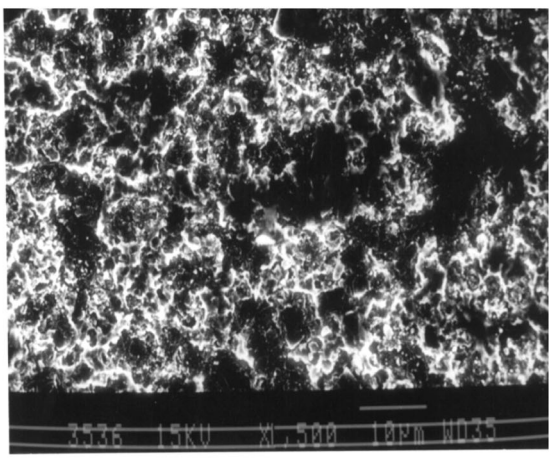

Figure 15 [Exp. No. 6]

Fig. 10–15 Microstructures of titanium work samples. Figures **10** (experiment no. 5), figure **11** (experiment no. 13), figure **12** (experiment no. 2), figure **13** (experiment no. 8), figure **14** (experiment no. 1), figure **15** (experiment no. 6)

fracture or fracture through cleavage of atomic planes. This could be identified from the numerous sharp edges and the elongated projected regions observed (Figs. 10, 11). In Fig. 11, large number of cracks can be observed along the grain boundaries indicating inter-granular fracture.

On the other hand, the experimental conditions corresponding to a medium level of energy input rate give rise to a mixed brittle fracture-plastic deformation mode of metal removal which is caused by significant amount of work hardening that takes place before the stuff fails. Figure 12 shows that an appreciable amount of localized plastic deformation took place and then the material finally failed by brittle fracture. This is evident from Fig. 13 (Experiment No. 8) that depicts the presence of some cleavage planes in addition to numerous even-sized dimples distributed in the entire surface.

From Figs. 14 and 15 (experiment no. 1, 6), a network consisting of large number of spherical dimples or microcavities with uniform shape and even distribution could be observed. This is clearly a sign of pure ductile failure of the work surface. Moreover, the white (brighter) contrast being observed in these figures gives an indication of the proportion of the surface that has been machined through ductile failure mode. The region represented by the dark (black) contrast is much less in proportion to the other region so the ductile failure is the predominant mode of metal removal at process conditions with low energy input rate.

There was no experimental evidence of any surface irregularity or disintegrity from the microstructure analysis. As already mentioned, as the process is free from temperature rise or any other thermal-based phenomenon (such as HAZ, recast layer, residual thermal stress) there is no appreciable change in the surface properties. This could prove very beneficial for the titanium components processed through USM as far as the longevity of the service life is concerned.

8 Practical applications of the work

The work reported in this paper would find application in the field of machining of commercially pure Titanium using ultrasonic machining. The findings may be very important for establishment of effective machining procedures for titanium, especially from the point of view of the surface integrity which includes the finish and the micro-hardness of the surface post machining. The results related to mode of material removal (brittle fracture and ductile failure) observed at different energy input conditions would enable the machinists to obtain a desired ratio of the two modes by systematically manipulating the input parametric conditions during machining. Moreover, the results reported in this investigation would add to the relatively scarce database on the machinability of titanium with non-conventional machining techniques.

9 Directions for future research

The velocity of the sound in a particular tool material in connection with the multiple of half wavelength of the vibration has to be considered for computation of the tool dimensions for ensuring that the total acoustic chain length corresponds to the resonant frequency. As a number of tool materials are involved in the research, having different characteristics of vibration transmission, this consideration is critical. In the present study, the effect of omitting this consideration while designing the tools has been resolved through randomization of experimental runs and fixing the tool weight to a preset value. However, the future research would be undertaken while including this important observation.

10 Conclusions

This research work is aimed at evaluation of the quality and micro-hardness of the machined surface for pure titanium samples using ultrasonic machining, to assess the potential of application of USM as a cost-effective alternative for commercial machining of titanium. Parametric optimization for surface roughness is obtained through planning and conducting the experiments using Taguchi's design of experiments approach. In addition, the multi-objective optimization of both response variables has been attempted using Taguchi's loss-function concept. To assess the effect of strain hardening on the sub-surface hardness of the machined samples, the hardness profile of machined samples at controlled experimental conditions (belonging to different energy input settings) has been constructed. The microstructures of the machined surface were also observed to identify and correlate the mode of failure with the energy input conditions.

In addition, following conclusions can be drawn from this investigation:

1. Under the range of parameters used in the investigation, best surface quality was realized while machining titanium workpiece with a tough and ductile tool material (titanium alloy), a softer abrasive for slurry preparation (brown alumina), very fine grit size of the abrasive (500, mean particle size 18 μm) and lowest level of power rating (100 W, 20 % of maximum power rating). The predicted optimum value of roughness (0.36 μm) was validated by conducting conformation experiments.
2. Considerable improvement has been realized in the surface roughness and micro-hardness through multi-objective optimization over the initial parameter setting. The multi-response *S*/*N* is also improved by

0.62 (over 20 %) improving the robustness at the optimized settings.

3. The desired mode of metal removal may be obtained, to the required level, by precisely controlling the energy input rate into the work surface through a systematic and controlled manipulation of input parameters.
4. Because of the plastic deformation due to repeated impacts of grains, the work surface experiences considerable amount of strain hardening. The micro-hardness gain after machining was measured under different machining conditions and was found to be inversely related to the rate of energy input to the workpiece. Micro-hardness gain was more for process conditions that dictate small machining rates or fine surface quality.
5. The relationship between surface roughness and micro-hardness of the machined surface was established through regression analysis. It was concluded that both the response variables were strongly correlated.
6. The effect of strain hardening has been found to limit to a sub-surface depth in the range of 150–250 μm, depending upon the parametric conditions at which the machining is performed. The depth of strain-hardened layer is more in case of process conditions involving higher energy input rates.

Acknowledgments The author would like to thank Mr. K. Ramesh (GM, MIDHANI, Hyderabad, India) and Mr. S.S. Arora (Punjab Abrasives, Mohalli, India) for providing necessary materials for the research work. The author is also thankful to Mr. Trilok Singh and Mr. Sukhdev Chand (Lab Superintendents, TU, Patiala) for providing laboratory facilities. The author feels indebted to Mr. Charlie Wilhite (Sonic-Mill, USA) for providing the accessories for USM apparatus and for giving invaluable guidance from time to time.

References

1. Kennedy DC, Grieve RJ (1975) Ultrasonic machining—A review. The Production. Engineer 54(9):481–486
2. Thoe TB, Aspinwall DK, Wise MLH (1998) Review on ultrasonic machining. Int J Mach Tools Manuf 38(4):239–255
3. Hong SY, Markus I, Jeong W (2001) New cooling approach and tool life improvement in cryogenic machining of titanium alloy Ti-6Al-4 V. Int J Mach Tools Manuf 41:2245–2260
4. Ezugwu EO, Wang ZM (1997) Titanium alloys and their machinability—a review. J Mater Process Technol 68(1–4): 262–274
5. Velasquez JD, Bolle B, Chevrier P, Geandier G, Tidu A (2007) Metallurgical study on chips obtained by high speed machining of Ti-6Al-4 V alloy. Mater Sci Eng 452–453:469–475
6. Wood RA, Favor RJ (1972) Titanium alloys handbook. Air Force Materials Laboratory, Ohio, pp 45–46
7. Amin AKM, Ismail AF, Khairusshima MK (2007) Effectiveness of uncoated WC/Co and PCD inserts in end milling of titanium alloy. J Mater Process Technol 192–193:147–158
8. Kremer, D.; (1991). New developments in ultrasonic machining. SME Technical Paper, (MR91-522) p 13
9. Kumar A, Kumar V, Kumar J (2013) Investigation of machining parameters and surface integrity in wire electric discharge machining of pure titanium. Proceedings of the Institution of Mechanical Engineers, Part B. J Eng Manuf 227(7):972–992. doi:10.1177/0954405413479791
10. Kumar A, Kumar V, Kumar J (2013) Multi-response optimization of process parameters based on response surface methodology for pure titanium using WEDM process. Int J Adv Manuf Technol 68(9–12):2645–2668. doi:10.1007/s00170-013-4861-9
11. Kumar A, Kumar V, Kumar J (2012) Prediction of surface roughness in wire electric discharge machining (wedm) process based on response surface methodology. Int J Eng Technol 2(4):708–719
12. Kumar A, Kumar V, Kumar J (2012) An Investigation into machining characteristics of commercially pure titanium (Grade-2) using CNC WEDM. Appl Mech Mater 159:56–68
13. Int ASM (1988) Titanium: a technical guide. ASM Int, Materials Park, pp 75–85
14. Moore D (1985). Ultrasonic impact grinding. Proceedings of. Non-Traditional machining Conference, Cinicinnati 137–139
15. Dvivedi A, Kumar P (2007) Surface quality evaluation in ultrasonic drilling through the Taguchi technique. Int J Adv Manuf Technol 34(1–2):131–140
16. Kumar J, Khamba JS, Mohapatra SK (2008) An investigation into the machining characteristics of titanium using ultrasonic machining. Int J Mach Mach Mater 3(1-2):143–161
17. Kumar J, Khamba JS, Mohapatra SK (2009) Investigating and modeling tool-wear rate in the ultrasonic machining of titanium. Int J Adv Manuf Technol 41(11):1101–1117
18. Kumar J, Khamba JS (2010) Modeling the material removal rate in ultrasonic machining of titanium using dimensional analysis. Int J Adv Manuf Technol 48(1–4):103–119
19. Kumar J, Khamba JS (2008) An experimental study on ultrasonic machining of pure titanium using designed experiments. J Braz Soc Mech Sci Eng 30(2):231–238
20. Kumar J, Khamba JS (2010) Multi-Response optimization in ultrasonic machining of titanium using Taguchi's approach and utility concept. Int J Manuf Res 5(2):1013–1022
21. Singh R, Khamba JS (2006) Ultrasonic machining of titanium and its alloys—a review. J Mater Process Technol 173(2):125–135
22. Singh R, Khamba JS (2007) Investigation for ultrasonic machining of titanium and its alloys. J Mater Process Technol 183(2–3):363–367
23. Benedict Gary F (1987) Non traditional manufacturing processes. Marcel Dekker Inc, New York
24. Gilmore, R.; (1989). Ultrasonic machining and orbital abrasion techniques. SME Technical Paper (series) AIR, (NM89-419) pp 1–20
25. Goetze D (1956) Effect of vibration amplitude, frequency, and composition of the abrasive slurry on the rate of ultrasonic machining in ketos tool steel. J Acoust Soc Am 28(6):1033–1045
26. Guzzo PL, Shinohara AH (2003) Ultrasonic abrasion of quartz crystals. Wear 255:67–77
27. Komaraiah M, Manan M, Reddy PN, Victor S (1988) Investigation of surface roughness and accuracy in ultrasonic machining. Precis Eng 10(2):59–68
28. Guzzo PL, Shinohara AH (2004) A comparative study on ultrasonic machining of hard and brittle materials. J Braz Soc Mech Sci Eng 26(1):56–64
29. Dam H, Quist P, Schreiber M (1995) Productivity, surface quality and tolerances in ultrasonic machining of ceramics. J Mater Process Technol 51(1–4):358–368
30. Koval Chenko MS, Paustovskii AV, Perevyazko VA (1986) Influence of properties of abrasive materials on the effectiveness of ultrasonic machining of ceramics. Powder Metall Met Ceram 25:560–562

31. Komariah M, Reddy PN (1993) Relative performance of tool materials in ultrasonic machining. Wear 161(1–2):1–10
32. Shaw MC (1956) Ultrasonic grinding. Annals of CIRP 5:25–53
33. Sharman AR, Aspinwall DK, Kasuga V (2001) Ultrasonic assisted turning of gamma titanium aluminide. In: Proceedings of 13th International Symposium for Electromachining, Spain, (Part-I) pp 939–951
34. Aspinwall DK, Kasuga V (2001) The use of ultrasonic machining for the production of holes in Y-TIAL.In: Proceedings of the 13th International Symposium for Electro machining ISEM XII vol 2. Spain, pp 925–937
35. Adithan M, Venkatesh VC (1976) Production accuracy of holes in ultrasonic drilling. Wear 40(3):309–318
36. Bagchi TP (1993) Taguchi methods explained: Practical steps to robust design. Prentice Hall of India Private Ltd, New York ISBN-0-87692-80804
37. Smith TJ (1973) Parameter influences in ultrasonic machining. Tribol Int 11(5):196–198
38. Mishra PK (2005) Non Conventional machining. Narosa Publishing House, New Delhi, pp 22–44 ISBN 81-7319-192-1
39. Markov AI (1959) Kinematics of the dimensional ultrasonic machining method. Mach Tool 30(10):28–31
40. Scab KHW (1990) Parametric studies of ultrasonic machining. SME Technical paper, (MR90-294) p 11
41. Springer C, Ahmed WU (1984) Metallographic preparation of titanium. Prakt Metallogr 21:200–203
42. Moreland MA (1988) Ultrasonic advantage revealed in the hole story. Appl Manuf 187:156–162
43. Jadoun RS (2009) Design of optimum process parameters for surface roughness in ultrasonic drilling (USD) of engineering ceramics using the Taguchi Method. J Mod Manuf Technol 2(1):29–48